Cell, Vol. 117, 323–335, April 30, 2004, Copyright ©2004 by Cell Press

Telomere Length Homeostasis Is Achieved via a Switch between Telomerase-Extendible and -Nonextendible States

M. Teresa Teixeira,[1,3] Milica Arneric,[1] Peter Sperisen,[2] and Joachim Lingner[1,*]
[1]Swiss Institute for Experimental Cancer Research and National Center of Competence in Research "Frontiers in Genetics"
[2]Swiss Institute for Bioinformatics
CH-1066 Epalinges/s Lausanne
Switzerland

Summary

Telomerase counteracts telomere erosion that stems from incomplete chromosome end replication and nucleolytic processing. A precise understanding of telomere length homeostasis has been hampered by the lack of assays that delineate the nonuniform telomere extension events of single chromosome molecules. Here, we measure telomere elongation at nucleotide resolution in *Saccharomyces cerevisiae*. The number of nucleotides added to a telomere in a single cell cycle varies between a few to more than 100 nucleotides and is independent of telomere length. Telomerase does not act on every telomere in each cell cycle, however. Instead, it exhibits an increasing preference for telomeres as their lengths decline. Deletion of the telomeric proteins Rif1 or Rif2 gives rise to longer telomeres by increasing the frequency of elongation events. Thus, by taking a molecular snapshot of a single round of telomere replication, we demonstrate that telomere length homeostasis is achieved via a switch between telomerase-extendible and -nonextendible states.

Introduction

The ends of eukaryotic chromosomes, known as telomeres, are essential protein-DNA complexes that protect chromosome ends from fusion and degradation (see Ferreira et al. [2004] for a recent review). The DNA component of telomeres typically comprises tandem repeats of simple sequences that are rich in guanosine residues in the strand containing the 3′ end, which protrudes to form a single strand overhang. Therefore, the recessed 5′ end-containing strand, which is replicated by the leading strand synthesis machinery, cannot function as a template for the synthesis of the 3′ overhang (Lingner et al., 1995). Hence, in the absence of special telomere maintenance mechanisms, linear chromosomes shorten progressively with every round of DNA replication. In addition, nucleolytic processing of telomere ends may contribute to shortening (Jacob et al., 2003; Wellinger et al., 1996). Telomere length limits the replicative potential of many normal human somatic cells (Bodnar et al., 1998).

The cellular reverse transcriptase telomerase counteracts telomere shortening (reviewed in Kelleher et al. [2002]). It extends the 3′ end of chromosomes by reverse transcribing in an iterative fashion the template region of its tightly associated telomerase RNA moiety. The complementary DNA strand is presumably synthesized by the conventional DNA polymerases α and δ (Diede and Gottschling, 1999; Ray et al., 2002). Telomerase expression is required for unlimited proliferation of unicellular organisms such as yeast or protozoa as well as for immortal cells in multicellular organisms such as germ cells, some stem cells, and many cancer cells. In humans, a decline in telomere length correlates with the onset of age-dependent mortality (Cawthon et al., 2003). Short telomeres and reduced levels of telomerase have been observed in individuals that carry a defective telomerase RNA gene or a defective allele of the telomerase-associated dyskerin protein (Mitchell et al., 1999; Vulliamy et al., 2001). Both genetic disorders give rise to the bone marrow failure syndromes dyskeratosis congenita and aplastic anemia, which may be caused by telomere exhaustion and a reduced replicative potential of stem cells. On the other hand, telomere length stabilization and upregulation of telomerase expression has fatal consequences during malignant transformation of cells that are normally telomerase negative (Kim et al., 1994).

In cells that express telomerase, the length of the duplex telomeric repeat array is kept within a species- and cell type-specific narrow range. In humans, the average telomere length varies between 5 and 15 kb, whereas in the yeast *S. cerevisiae*, telomere length is around 300 nucleotides. Telomere length homeostasis is the result of a balance between telomere shortening and telomere lengthening activities (see Smogorzewska and de Lange [2004] for a recent review). As discussed above, a primary cause of telomere shortening is incomplete DNA end replication. Nucleolytic processing of telomere ends is presumably important for the generation of 3′ overhangs, which are present on both chromosomal ends (Huffman et al., 2000; Makarov et al., 1997; McElligott and Wellinger, 1997; Wellinger et al., 1996; Wright et al., 1997). The telomere shortening rate in the absence of telomerase is insensitive to telomere length and corresponds to 50–200 nucleotides per round of DNA replication in human cells and three nucleotides per generation in *S. cerevisiae* (Harley et al., 1990; Huffman et al., 2000; Lundblad and Szostak, 1989; Marcand et al., 1999). Telomere shortening can also occur in a more stochastic fashion through so-called telomeric rapid deletions (TRD), which involve intrachromatid recombination events (Bucholc et al., 2001; Li and Lustig, 1996).

Telomere lengthening requires telomerase in most species. However, under rare circumstances, recombination-mediated pathways may maintain telomeres in the absence of telomerase (Bryan et al., 1995; Dunham et al., 2000; Lundblad and Blackburn, 1993; Teng and Zakian, 1999). This is observed at low frequency in yeast cells that escape the lethality caused by telomerase loss and in some in vitro-immortalized and cancer-derived

*Correspondence: joachim.lingner@isrec.unil.ch
[3]Present address: Institut Pasteur, 75724 Paris Cedex 15, France.

human cell lines. The contribution of recombination to telomere length maintenance in wt cells is unknown.

In *S. cerevisiae*, telomerase extends telomeres in late S phase (Marcand et al., 2000), and this is thought to be coupled to semiconservative DNA replication (Diede and Gottschling, 1999). Numerous gene products have been implicated in telomere maintenance. Mutations in some of these genes abolish telomerase activity, leading to progressive telomere shortening. Telomere replication factors that are essential in vivo include telomerase subunits and proteins that bind to the telomeric 3′ overhang, where they mediate the access and activation of telomerase (reviewed by Evans and Lundblad [2000]). ATM- and ATR-related protein kinases are also required for telomerase activity in vivo in fission and budding yeast (Naito et al., 1998; Ritchie et al., 1999), but their critical substrates are yet to be identified. Mutations in other telomeric factors perturb but do not abolish the end replication machinery, leading to an altered steady-state telomere length. For example, some double-stranded telomeric DNA binding proteins are negative regulators of telomere length. Budding yeast Rap1p is a major component of telomeric chromatin (reviewed by Shore [1997]) that binds the telomeric repeats with high affinity and negatively affects telomere length (Lustig et al., 1990; Conrad et al., 1990). Through a C-terminal domain, Rap1p recruits two proteins, Rif1p and Rif2p, which contribute to telomere length control (Hardy et al., 1992; Wotton and Shore, 1997). Targeting of additional copies of the Rap1p C terminus to a telomere induces telomere shortening to an extent that is roughly proportional to the number of targeted molecules (Marcand et al., 1997; Ray and Runge, 1999b). This observation led to the "protein counting model" of telomere length control (Marcand et al., 1997), in which telomerase-mediated telomere extension is regulated by the number of telomere bound Rap1p molecules. Additional support for a counting mechanism comes from work with telomerase RNA template mutants in *S. cerevisiae* and the related yeast *Kluveromyces lactis* (Chan et al., 2001; McEachern and Blackburn, 1995). Such mutations reduced the number of telomeric binding sites for Rap1p and concomitantly induced massive telomere elongation. The protein-counting model was also supported by measurement of the reelongation kinetics of an artificially shortened telomere (Marcand et al., 1999). These experiments indicated that the rate of telomere elongation is inversely proportional to telomere length.

Double-stranded telomere binding proteins in fission yeast and vertebrates also function as negative regulators of telomere length, similarly to *S. cerevisiae* Rap1p. Disruption of the fission yeast *taz1* gene gives rise to a 10-fold increase in telomere length (Cooper et al., 1997), and depletion of the orthologous human TRF1 from telomeres also leads to substantial telomere lengthening (van Steensel and de Lange, 1997). Overexpression of TRF1 induces telomere shortening without affecting telomerase activity in vitro (Smogorzewska et al., 2000). Similarly, the TRF1-interacting proteins TIN2 and tankyrase 1 regulate telomere length without affecting telomerase activity in vitro (Kim et al., 1999; Smith and de Lange, 2000). These experiments suggest that telomerase is regulated by the telomeric substrate in *cis*. Consistent with this notion, artificial tethering of TRF1 to a specific telomere induced its shortening in *cis* (Ancelin et al., 2002). Evidence for regulation of telomerase activity in *cis* had been provided even earlier in telomere healing experiments in which newly seeded telomeres were smaller than the endogenous telomeres (Barnett et al., 1993). Furthermore, in mice, crosses between strains with short and long telomeres result in a preferential elongation of short telomeres (Zhu et al., 1998; Hemann et al., 2001; Samper et al., 2001). Similarly, expression of limiting amounts of telomerase activity in human fibroblasts leads to preferential elongation of short telomeres (Ouellette et al., 2000).

At least two not mutually exclusive models could provide a mechanistic basis for the protein-counting model of telomere length control and the increased activity of telomerase on shorter telomeres. First, the elongation efficiency of telomerase, i.e., the number of nucleotides added to an individual telomere per elongation event, could be regulated as a function of telomere length. Thus, all telomeres would be available for telomerase-mediated extension, but the telomere structure would regulate the catalytic activity of telomerase in a length-dependent manner, perhaps by influencing the processivity or turnover of the enzyme. Second, the productive association of telomerase with telomere 3′ ends could be regulated by length-dependent changes in telomeric chromatin structure. A long telomere would have a lower probability to be in a telomerase-extendible state than a short telomere. In this model, a telomere could shorten for several rounds of DNA replication without being elongated by telomerase, before its chromatin structure would switch and become competent for telomerase-mediated elongation. Thus, the association, rather than the activity, of telomerase would be the regulated element.

To distinguish between these two models, we devised a system to measure elongation of single telomeres in vivo at nucleotide resolution. Using this system, we determined the frequency and elongation efficiency of telomeres as a function of their length. We find that telomere elongation is a stochastic process that does not occur at all telomeres in every cell cycle. Short telomeres have a higher probability of being extended than long telomeres. A variable number of telomeric repeats can be added in one round of replication to a single chromosome end, but the number of added nucleotides does not correlate with telomere length, unless the telomere is almost completely eroded. The frequency of telomerase-mediated extension increases in *rif1*-Δ and *rif2*-Δ mutants. Taken together, our results provide direct evidence for a model in which telomeres switch in a length-dependent manner between at least two structural states that dictate the extendibility by telomerase.

Results

An Assay for Measuring Single Telomere Extension at Nucleotide Resolution In Vivo

To study the mechanisms that control telomere access and extension efficiency, we developed a system to measure single telomere elongation events in vivo at nucleotide resolution in *S. cerevisiae* (Figure 1). A telomerase-negative strain was created by deleting the

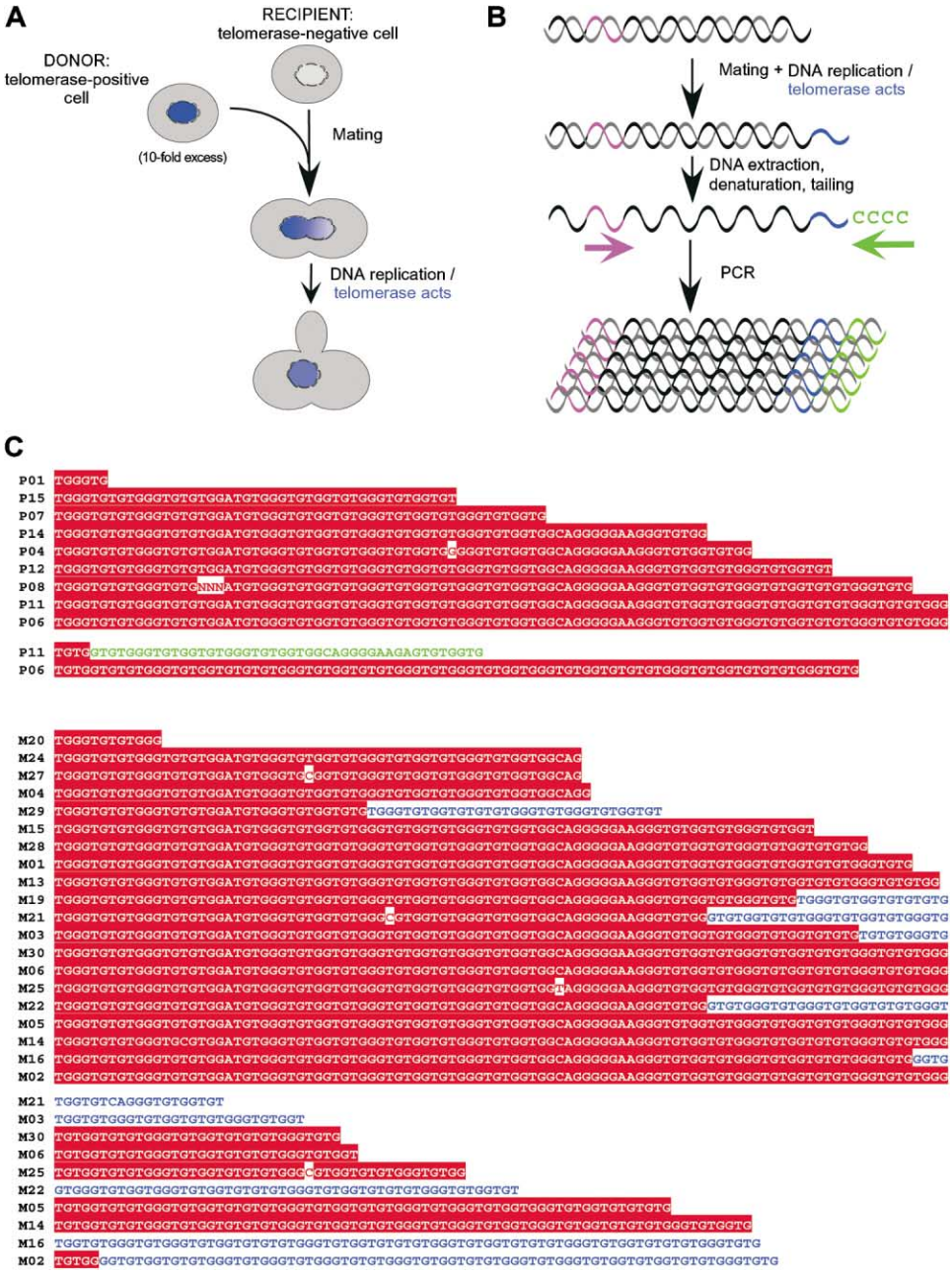
A
RECIPIENT:
telomerase-negative cell
DONOR:
telomerase-positive
cell
(10-fold excess)
Mating
DNA replication /
telomerase acts
B
Mating + DNA replication /
telomerase acts
DNA extraction,
denaturation, tailing
CCCC
PCR
C
P01 TGGGTG
P15 TGGGTGTGTGGGTGTGTGGATGTGGGTGTGGTGTGGGTGTGGTGT
P07 TGGGTGTGTGGGTGTGTGGATGTGGGTGTGGTGTGGGTGTGGTGTGGGTG
P14 TGGGTGTGTGGGTGTGTGGATGTGGGTGTGGTGTGGGTGTGGTGTGGGTGTGGTGGCAGGGGGAAGGGTGTGG
P04 TGGGTGTGTGGGTGTGTGGATGTGGGTGTGGTGTGGGTGTGGTGCGGGTGTGGTGGCAGGGGGAAGGGTGTGGTGTGG
P12 TGGGTGTGTGGGTGTGTGGATGTGGGTGTGGTGTGGGTGTGGTGTGGGTGTGGTGGCAGGGGGAAGGGTGTGGTGTGGGTGTGGTGT
P08 TGGGTGTGTGGGTGTCNNNATGTGGGTGTGGTGTGGGTGTGGTGTGGGTGTGGTGGCAGGGGGAAGGGTGTGGTGTGGGTGTGGTGTGTGGGTGTG
P11 TGGGTGTGTGGGTGTGTGGATGTGGGTGTGGTGTGGGTGTGGTGTGGGTGTGGTGGCAGGGGGAAGGGTGTGGTGTGGGTGTGGTGTGTGGGTGTGTGGG
P06 TGGGTGTGTGGGTGTGTGGATGTGGGTGTGGTGTGGGTGTGGTGTGGGTGTGGTGGCAGGGGGAAGGGTGTGGTGTGGGTGTGGTGTGTGGGTGTGTGGG

P11 TGTGGTGTGGGTGTGGTGTGGGTGTGGTGGCAGGGGAAGAGTGTGGTG
P06 TGTGGTGTGTGGGTGTGGTGTGTGTGGGTGTGGTGTGTGGGTGTGGGTGTGGTGGGTGTGGTGTGTGTGGGTGTGGTGTGTGTGGGTGTG

M20 TGGGTGTGTGGG
M24 TGGGTGTGTGGGTGTGTGGATGTGGGTGTGGTGTGGGTGTGGTGTGGGTGTGGTGGCAG
M27 TGGGTGTGTGGGTGTGTGGATGTGGGTGCGGTGTGGGTGTGGTGTGGGTGTGGTGGCAG
M04 TGGGTGTGTGGGTGTGTGGATGTGGGTGTGGTGTGGGTGTGGTGTGGGTGTGGTGGCAGG
M29 TGGGTGTGTGGGTGTGTGGATGTGGGTGTGGTGTCTGGGTGTGGTGTGTGTGGGTGTGGGTGTGGTGT
M15 TGGGTGTGTGGGTGTGTGGATGTGGGTGTGGTGTGGGTGTGGTGTGGGTGTGGTGGCAGGGGGAAGGGTGTGGTGTGGGTGTGGT
M28 TGGGTGTGTGGGTGTGTGGATGTGGGTGTGGTGTGGGTGTGGTGTGGGTGTGGTGGCAGGGGGAAGGGTGTGGTGTGGGTGTGGTGTGTGG
M01 TGGGTGTGTGGGTGTGTGGATGTGGGTGTGGTGTGGGTGTGGTGTGGGTGTGGTGGCAGGGGGAAGGGTGTGGTGTGGGTGTGGTGTGTGGGTGTG
M13 TGGGTGTGTGGGTGTGTGGATGTGGGTGTGGTGTGGGTGTGGTGTGGGTGTGGTGGCAGGGGGAAGGGTGTGGTGTGGGTGTGGTGTGTGGGTGTGTGG
M19 TGGGTGTGTGGGTGTGTGGATGTGGGTGTGGTGTGGGTGTGGTGTGGGTGTGGTGGCAGGGGGAAGGGTGTGGTGTGGGTGTGTGGGTGTGTGTG
M21 TGGGTGTGTGGGTGTGTGGATGTGGGTGTGGTGTGGCGTGGTGTGGGTGTGGTGGCAGGGGGAAGGGTGTGCGTGTGGTGTGTGGGTGTGGTGTGGGTG
M03 TGGGTGTGTGGGTGTGTGGATGTGGGTGTGGTGTGGGTGTGGTGTGGGTGTGGTGGCAGGGGGAAGGGTGTGGTGTGGGTGTGGTGTGTCTGTGTGGGTG
M30 TGGGTGTGTGGGTGTGTGGATGTGGGTGTGGTGTGGGTGTGGTGTGGGTGTGGTGGCAGGGGGAAGGGTGTGGTGTGGGTGTGGTGTGTGGGTGTGGG
M06 TGGGTGTGTGGGTGTGTGGATGTGGGTGTGGTGTGGGTGTGGTGTGGGTGTGGTGGCAGGGGGAAGGGTGTGGTGTGGGTGTGGTGTGTGGGTGTGTGGG
M25 TGGGTGTGTGGGTGTGTGGATGTGGGTGTGGTGTGGGTGTGGTGTGGGTGTGGTGGTAGGGGGAAGGGTGTGGTGTGGGTGTGGTGTGTGGGTGTGTGGG
M22 TGGGTGTGTGGGTGTGTGGATGTGGGTGTGGTGTGGGTGTGGTGTGGGTGTGGTGGCAGGGGGAAGGGTGTGCGTGTGGGTGTGGTGTGTGGGTGTGGGT
M05 TGGGTGTGTGGGTGTGTGGATGTGGGTGTGGTGTGGGTGTGGTGTGGGTGTGGTGGCAGGGGGAAGGGTGTGGTGTGGGTGTGGTGTGTGGGTGTGTGGG
M14 TGGGTGTGTGGGTGCGTGGATGTGGGTGTGGTGTGGGTGTGGTGTGGGTGTGGTGGCAGGGGGAAGGGTGTGGTGTGGGTGTGGTGTGTGGGTGTGTGGG
M16 TGGGTGTGTGGGTGTGTGGATGTGGGTGTGGTGTGGGTGTGGTGTGGGTGTGGTGGCAGGGGGAAGGGTGTGGTGTGGGTGTGGTGTGTGGGTGTGGGTG
M02 TGGGTGTGTGGGTGTGTGGATGTGGGTGTGGTGTGGGTGTGGTGTGGGTGTGGTGGCAGGGGGAAGGGTGTGGTGTGGGTGTGGTGTGTGGGTGTGTGGG

M21 TGGTGTCAGGGTGTGGTGT
M03 TGGTGTGGGTGTGGTGTGTGGGTGTGGT
M30 TGTGGTGTGTGGGTGTGGTGTGTGTGGGTGTG
M06 TGTGGTGTGTGGGTGTGGTGTGTGTGGGTGTGGT
M25 TGTGGTGTGTGGGTGTGGTGTGTGTGGGCGTGGTGTGTGGGTGTGG
M22 GTGGGTGTGGTGGGTGTGGTGTGTGTGGGTGTGGTGTGTGTGGGTGTGGTGT
M05 TGTGGTGTGTGGGTGTGGTGTGTGTGGGTGTGGTGTGTGGGTGTGGGTGTGGTGGGTGTGGTGTGTGTG
M14 TGTGGTGTGTGGGTGTGGTGTGTGGGTGTGGTGTGTGGGTGTGGGTGTGGTGGGTGTGGTGTGGGTGTGGTG
M16 TGGTGTGGGTGTGGGTGTGGTGTGTGTGGGTGTGGTGTGTGTGGGTGTGGTGTGTGTGGGTGTGGTGTGTGTGGGTGTG
M02 TGTGGGGTGTGGTGTGTGGGTGTGGGTGTGGGTGTGTGGGTGTGGTGTGTGGGTGTGGGTGTGGTGTGGTGTGTGGGTGTG

Figure 1. An Experimental System for Measuring Telomere Extension In Vivo at Nucleotide Resolution

(A) Introduction of telomerase activity in a controlled fashion to a telomerase-negative cell by functional complementation. Clonal telomerase-negative cells (recipients) are mated with telomerase-positive cells (donors) of the opposite mating type. Upon karyogamy, the newly formed zygotes enter their first S phase, and telomerase from the donor cell can elongate shortened telomeres inherited from the telomerase-negative recipients.

(B) Specific amplification of telomere VR of the recipient strain by telomere PCR (Forstemann et al., 2000; see Experimental Procedures). DNA is extracted from the zygotes, and DNA ends are tailed with terminal transferase and dCTP (green). Telomere VR of the recipient contains a unique sequence in the subtelomeric region (purple). This allows specific amplification by PCR with a primer that anneals to the sequence tag and a primer that is complementary to the oligo-dC tail. Telomerase-mediated telomere DNA extension is indicated by the blue line.

(C) Sequence alignment of telomere VR from a recipient clonal population before mating (P; upper alignment) and 3 hr after mating (M; lower alignment). Telomere extension events are detected by sequence divergence that arises among sister telomeres due to the action of yeast telomerase, which adds imperfect telomeric repeats (blue letters). Most sister telomeres that stem from the telomerase-negative parent are identical in sequence, because they are replicated faithfully by the semiconservative DNA replication machinery. They only differ in length due to irregular shortening. One out of nine parental telomeres analyzed (P11) diverged in sequence in the telomerase-negative clonal population. This is due to a telomerase-independent telomere rearrangement (green). N, ambiguous bases.

telomerase RNA gene *TLC1*. An isolated *tlc1*-Δ colony was grown for approximately 30 generations. Active telomerase was provided by mating the *tlc1*-Δ strain (referred to as "recipient") with a telomerase-positive strain (referred to as "donor") of the opposite mating type (Figure 1A). Thus, telomeres that had shortened in the telomerase-negative parent become reextended in the zygote due to the presence of complementing telomerase. Telomere elongation was detected by cloning and sequencing telomeres that originated from the recipient. To this end, we used as recipient a strain harboring the *ADE2* gene in the subtelomeric region of chromosome VR, which served as a sequence tag. Telomere VR was amplified by telomere PCR as described (Forstemann et al., 2000, and Figure 1B). In this method, genomic DNA is isolated and tailed in vitro with dCTP and terminal transferase. Telomere VR is amplified specifically with a primer that anneals with the *ADE2* gene at VR and a primer that is complementary to the oligo dC tail. PCR products were resolved on agarose gels, cloned, and sequenced (see Experimental Procedures). Yeast telomerase adds imperfect 5′-$(TG)_{0-6}$TGGGTG TG(G)-3′ repeats (Forstemann and Lingner, 2001). Thus, telomere elongation is detectable via the divergence of telomeric sequences in the telomere-distal region relative to the telomeric DNA synthesized by semiconservative DNA replication, which does not vary during clonal expansion. Thus, even if two telomere extension events occurred at the same nucleotide, they can be distinguished due to tract divergence. A representative example is given in Figure 1C, in which telomere VR was amplified, cloned, sequenced, and aligned in the *tlc1*-Δ parental strain after propagation for approximately 30 generations without telomerase and from the *tlc1*-Δ/*TLC1* zygote 3 hr after mating. The frequency of telomeres showing sequence divergence in the mating mixture was significantly increased compared to the parental telomeres, allowing us to examine telomerase-dependent telomere extensions at nucleotide resolution.

Telomerase Does Not Extend Every Telomere in Every Cell Cycle

To correlate telomere elongation kinetics with zygote formation and subsequent cell divisions, time course experiments were performed (Figure 2). Mating was followed by plating on selective media to assess the presence of auxotrophic markers (Figure 2A) by cytological observation (Figure 2B) and by fluorocytometric (FACS) analysis of DNA content (Figure 2C). Mating efficiency was quantified and optimized to nearly 100% by collecting the telomerase-negative strain together with a 10-fold excess of the telomerase-positive strain on filter papers (see Experimental Procedures). Microscopic analysis and assessment of auxotrophic markers indicated that almost all recipient cells had initiated cell-to-cell contact and zygote formation after approximately 2 hr. At this time point, most cells were in G1, as determined by FACS (Figure 2C). After 3 hr, approximately 9% of the cells contained a 4C DNA content (Figure 2C). Because of the 10-fold excess of wt over *tlc1*-Δ haploids, this was consistent with the notion that, at this time point, most zygotes had completed a single S phase. After approximately 3.5 hr, the diploid cell number had doubled, indicating that most diploids had undergone mitosis and completed one cell cycle (Figure 2A). The combined analyses indicated that zygote formation and the subsequent S phase occurred with high synchrony and that, 3 hr after initial mixing, most zygotes had completed their first round of DNA replication.

Telomere VR was amplified by telomere PCR (Figure 2D) and cloned from the parental *tlc1*-Δ strain and from the *tlc1*-Δ/*TLC1* diploid 3, 5, and 7 hr postmating. Telomere sequence analysis (Figure 2E) indicated that during the time course experiment, the fraction of telomere extension events increased. After 3 hr, which corresponds to a time point when most zygotes had completed one S phase, nine out of 25 (36%) sequenced telomeres had been elongated. After 5 hr, the ratio of extended to nonextended telomeres was roughly maintained (nine out of 22 = 40%), whereas after 7 hr, or approximately three population doublings, 10 out of 11 telomeres were elongated. This experiment demonstrates that not all telomeres become extended by telomerase in every cell cycle, even if they are considerably shorter than wt.

Telomerase-Independent Lengthening of Chromosome Ends

Inspection of telomere sequences in *tlc1*-Δ parents (Figure 2E) revealed that, even in the absence of telomerase, one out of ten telomere 3′ ends diverged in sequence from their sisters. To quantify these telomerase-independent elongation events, we cloned and sequenced the telomeres from haploid (Figures 3A–3C) and diploid (Figures 3D and 3E) telomerase-negative strains that lacked either *TLC1* or *EST1*. *EST1* encodes a telomerase-associated protein that is essential for telomerase activity in vivo, but it is not required for in vitro activity. Est1p has been implicated in recruitment and activation of telomerase at chromosomal ends (Evans and Lundblad, 1999; Pennock et al., 2001; Taggart et al., 2002). Sequence analysis of VR telomeres revealed that telomerase-independent elongation events occurred at similar rates in all four telomerase-negative strains. Thirty generations of clonal expansion resulted in 6.6% (13 out of 197 at VR) telomeres showing this type of event. Involved telomeres were variable in size from 41 to 226 nucleotides, and elongations varied from three to 179 nucleotides. Thus, these telomerase-independent extension events occurred prior to achievement of critical telomere shortening. We suspect that the divergence is due to recombination events involving TG repeats of different chromosome ends.

Variability of Telomere Extension Length

To analyze the relationship between telomere length and telomerase activity in vivo, we quantified the telomere elongation events that occurred after one round of DNA replication following telomerase reintroduction in *tlc1*-Δ/*TLC1* zygotes and in *est1*-Δ/*EST1* zygotes (Figure 4). In order to achieve an extensive coverage of telomere lengths, we performed the mating experiments with several independent clones for each strain. Figures 4A and 4B show the results of independent experiments in which the tagged telomere VR had a different length

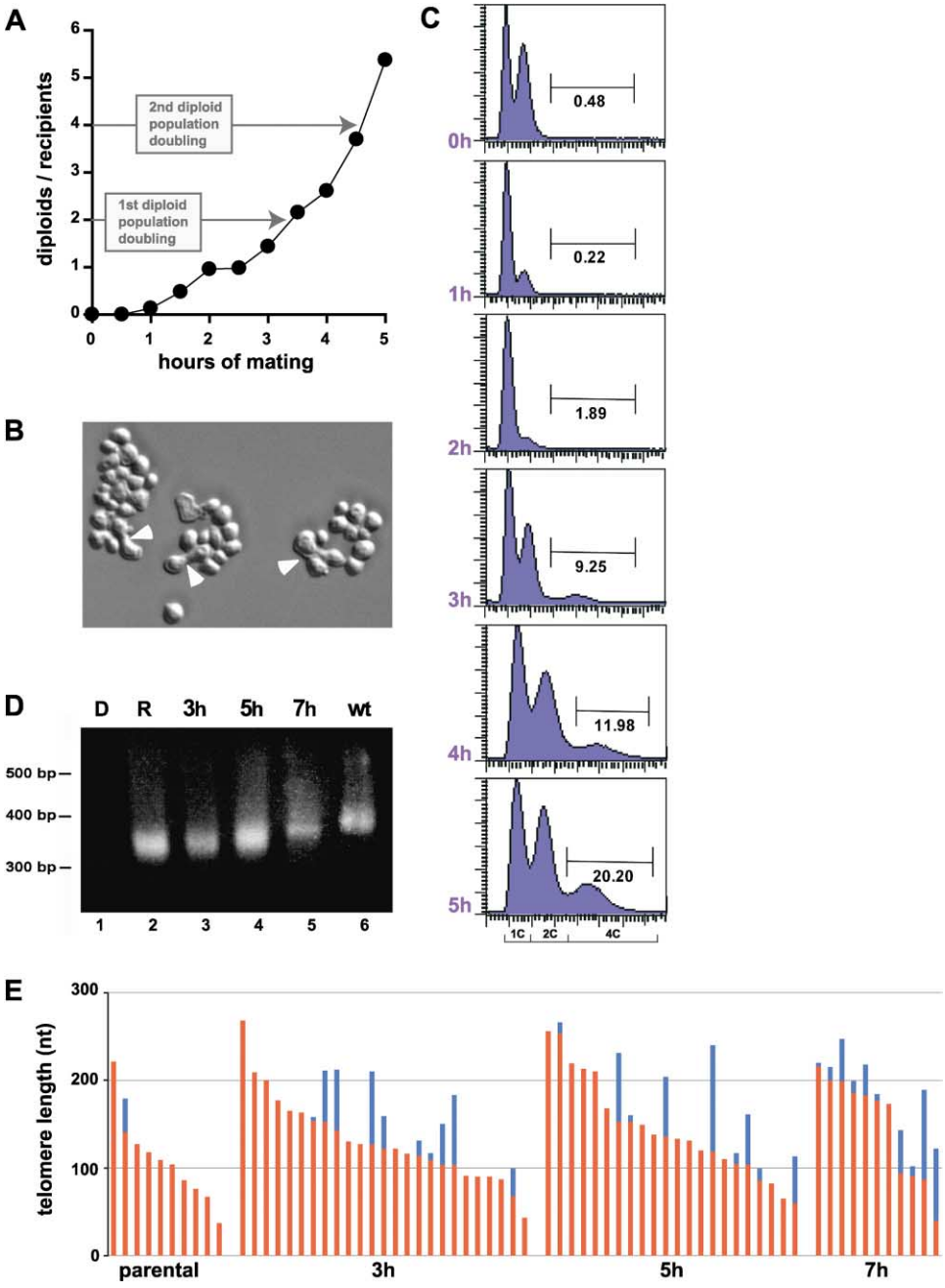

Figure 2. Time Course Experiment of Telomere Elongation and Cell Cycle Progression

(A) Mating efficiency and cell cycle progression as determined by plating on selective media. The ratio of diploids to recipients is plotted as a function of time. Mating was performed under standard conditions but with two telomerase-positive strains to allow efficient colony formation. In order to determine the number of haploid recipient cells and mated diploids, cultures were plated on medium lacking either histidine or histidine and leucine. Colonies were counted after 2 days at 30°C.

(B) Estimation of mating efficiency by counting zygotes under the microscope (Nomarski) after 3 hr. Zygotes are indicated with white arrowheads.

(C) Measurement of DNA content by fluorocytometry. DNA content of cells was measured for 5 hr following the initial mixing. The percentage of cells with a 4C content, which corresponds to the duplication of a diploid genome, is indicated.

(D) Amplification of telomere VR by telomere PCR. Telomere VR was amplified from the telomerase-negative recipient strain YT48/*tlc1*-Δ before mating (lane 2) and 3, 5, and 7 hr after mating (lanes 3–5) with the telomerase-positive donor strain FYBL1-23D (lane 1). The telomere PCR product of YT48 DNA is shown in lane 6.

(E) Analysis of telomere PCR products. Telomere PCR products corresponding to (D) were cloned, sequenced, and analyzed as described in Experimental Procedures. Individual telomeres from the recipient culture (parental) and from mated cultures (3, 5, and 7 hr after initial mixing) are represented by the vertical bars. The red part indicates the telomeric region, which is nondiverging. The blue part indicates the telomeric region that diverged among the sisters due to telomere extension.

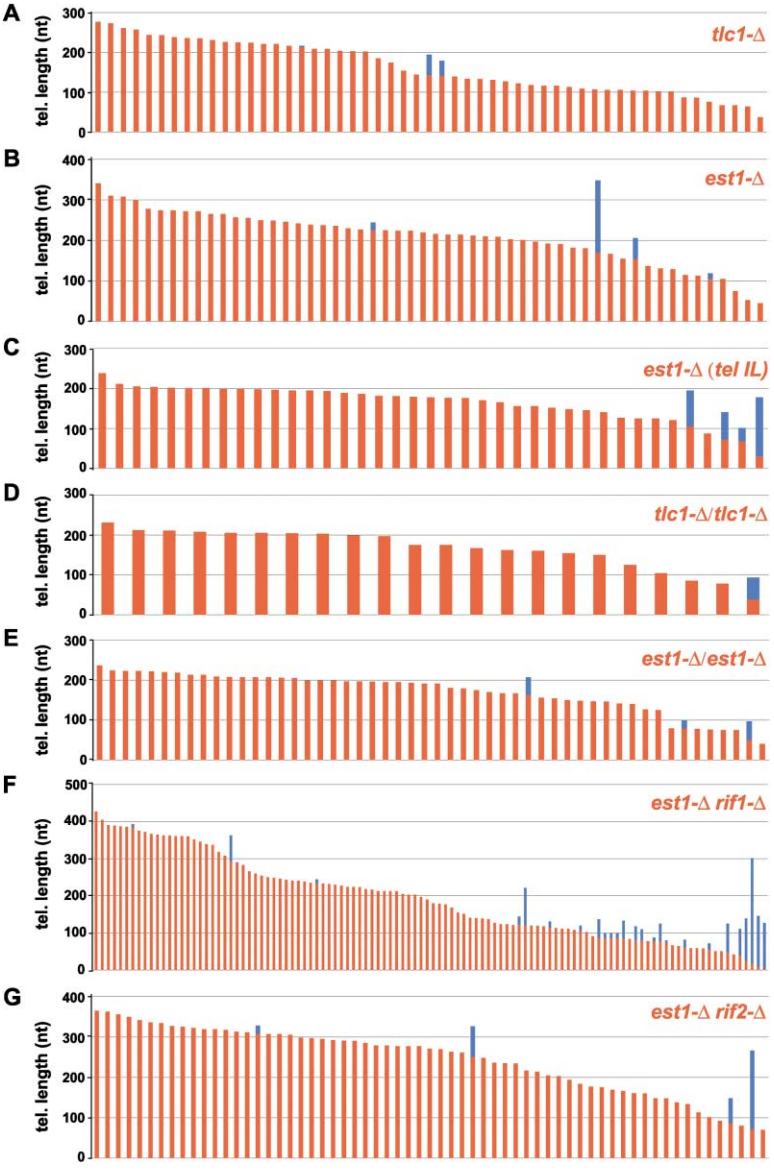

Figure 3. Telomerase-Independent Telomere Extension

Telomere VR (A, B, and D–G) and telomere 1L (C) were PCR amplified and analyzed as in Figure 2 from clonal populations after 30 cell doublings from YT48/*tlc1*-Δ cells (A), YT48/*est1*-Δ cells (B and C), diploid *tlc1*-Δ/*tlc1*-Δ (C), diploid *est1*-Δ/*est1*-Δ cells (D), *est1*-Δ *rif1*-Δ cells (F), and *est1*-Δ *rif2*-Δ cells (G).

when reextended by the complementing telomerase in the zygote. To analyze elongation events at telomeres of wt length, we analyzed a strain in which telomeres were overelongated before telomerase removal and mating (Figure 4B, left). To do this, we transformed the recipient *est1*-Δ strain with plasmid pVL1120 expressing a fusion protein between the DNA binding domain of Cdc13p and Est1p (Est1-DBD_{Cdc13}), a construct that complements *est1*-Δ and leads to telomere overelongation (Evans and Lundblad, 1999). Upon culturing the *est1*-Δ/pVL1120 strain for 50 generations under selection for the plasmid, the strain was plated on nonselective YPD medium. Cells that had lost pVL1120 were telomerase negative and were mated as above with a telomerase-positive wt strain for 3 hr.

After 3 hr of mating, most of the resulting zygotes were in G2 following their first round of DNA replication. Strikingly, the telomere extensions were very heterogeneous in size, ranging from four to 187 nucleotides in *tlc1*-Δ/*TLC1* zygotes and from four to 417 nucleotides in *est1*-Δ/*EST1* zygotes. The average extension length in *tlc1*-Δ/*TLC1* cells was 45 nucleotides, with an interquartile range from 14 to 66 nucleotides (Table 1). In *est1*-Δ/*EST1* cells, the average extension length was 86 nucleotides, with an interquartile range from 14 to 80 nucleotides. The longer average seen in *est1*-Δ/*EST1* zygotes stems from very long extension events of extremely short telomeres (Figure 4B and Table 1). As the mean telomeric repeat length in *S. cerevisiae* is 12–13 nucleotides (Forstemann and Lingner, 2001), telomere extension length corresponded in the majority of cases to several telomeric repeats. Thus, the in vivo properties of yeast telomerase differ markedly from its biochemical properties in vitro, where it performs only one elongation cycle and prevents further elongation by stably associating with the telomeric primer (Cohn and Blackburn, 1995; Prescott and Blackburn, 1997).

Surprisingly, the number of added nucleotides is not correlated significantly with telomere length (Figure 4D) (*tlc1*-Δ/*TLC1*: $r = -0.29$, $p_{pearson} = 0.15$; $\rho = -0.27$,

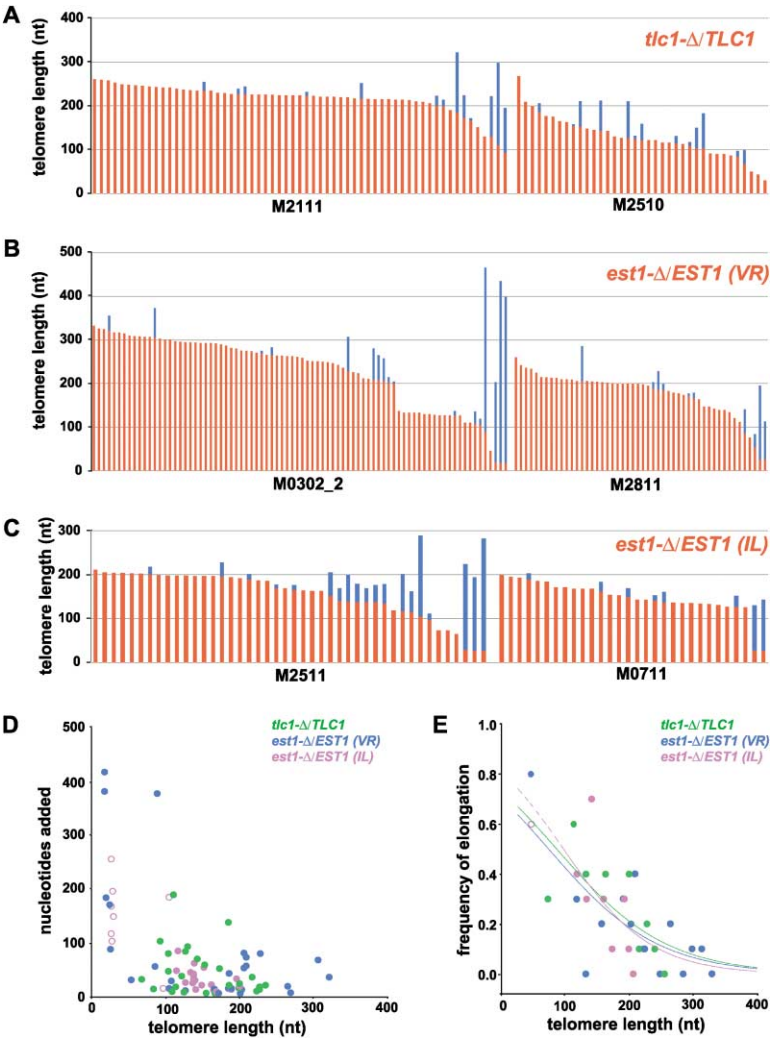

Figure 4. Frequency and Length of Telomere Extension as a Function of Telomere Size

(A) Telomere elongation events in *tlc1*-Δ/*TLC1* zygotes. YT48/*tlc1*-Δ cells were mated with FYBL1-23D cells for 3 hr. The tagged telomere at VR (tel VR::ADE2) was amplified, cloned, and sequenced. Two independent experiments (M2111 and M2510) are depicted on the left and right sides. Labeling is as in Figure 2.

(B) Telomere VR elongation events in *est1*-Δ/*EST1* zygotes. YT57/*est1*-Δ (left side, M0302_2) and YT48/*est1*-Δ (right side, M2811) cells were mated with FYBL1-23D as in (A).

(C) Elongation events at the natural telomere IL in *est1*-Δ/*EST1* zygotes. YT48/*est1*-Δ cells were mated with MAY01 for 3 hr. MAY01 lacks the subtelomeric region at telomere IL. Two independent experiments (M2511 and M0711) are depicted on the left and right sides.

(D) Length of telomere extension as function of telomere size. The sizes of diverging regions obtained in the experiments described in (A), (B), and (C) are plotted as a function of the nondiverging sequence, which corresponds to the length of the original telomere. Green dots indicate events from (A), blue dots events from (B), and pink dots from (C). Pink circles indicate events that could not be attributed without ambiguity to telomerase-mediated extension due to the high recombination background for short telomeres at chromosome 1L in the parent (see Figure 3C).

(E) Frequency of telomere extension as function of telomere size. Sequences obtained from (A), (B), and (C) were ordered according to nondiverging telomere size and pooled into subgroups containing ten telomeres each. The frequency of elongation in each subgroup was calculated and plotted as a function of telomere length. Data points were fitted to the following logistic regression model: $[(\text{frequency of elongation}) \sim \beta_0 + \beta_1 (\text{mean length}) + \epsilon]$. The $p_{\beta 1}$ value for *tlc1*-Δ/*TLC1* zygotes is 0.00447; for *est1*-Δ/*EST1* (at the tagged telomere VR), 0.00018; and for *est1*-Δ/*EST1* (at the natural telomere IL), 0.00592. The curve corresponding to *est1*-Δ/*EST1* (telomere 1L) is dashed for telomeres below 100 nt, because, in this region, the events could not be attributed with high confidence to telomerase-mediated extension, due to the high recombination background for short telomeres at chromosome 1L in the parent (see Figure 3C).

$p_{spearman} = 0.19$; *est1*-Δ/*EST1*: $r = -0.37$, $p_{pearson} = 0.062$; $\rho = -0.37$, $p_{spearman} = 0.059$). However, extremely long extensions of several hundred nucleotides were observed with very short telomeres of less than 100 nucleotides, indicating loss of normal telomerase control.

Telomerase Acts Preferentially on Short Telomeres

To determine whether the frequency of telomere elongation was regulated by telomere size, we sorted telomeres according to the length of their nondiverging telomeric sequence and formed subgroups containing ten telomeres each. The average telomere size of each subgroup was calculated, and the frequency of elongation in each subgroup was plotted as a function of telomere length (Figure 4E). Although the data scattered substantially, the frequency of elongation correlated significantly with telomere size (*tlc1*-Δ/*TLC1*: $r = -0.75$, $p_{pearson} = 0.0125$, $\rho = -0.80$, $p_{spearman} = 0.0082$; *est1*-Δ/*EST1*: $r = -0.70$, $p_{pearson} = 0.0057$, $\rho = -0.59$, $p_{spearman} =$

Table 1. Comparison of Telomere Elongation Lengths in *tlc1*-Δ/*TLC1*, *est1*-Δ/*EST1*, *est1*-Δ/*EST1 rif1*-Δ/*rif1*-Δ, and *est1*-Δ/*EST1 rif2*-Δ/*rif2*-Δ Zygotes

Average (Interquartile Range)			
Original telomere length	<100 nt	>200 nt	all
tlc1-Δ/*TLC1*	49 (22–67)	19 (13–22)	45 (14–66)
est1-Δ/*EST1*	212 (79–378)	44 (15–70)	86 (14–80)
est1-Δ/*EST1 (tel IL)*	NA	ND	67 (21–93)
est1-Δ/*EST1 rif1*-Δ/*rif1*-Δ	NA	59 (31–78)	NA
est1-Δ/*EST1 rif2*-Δ/*rif2*-Δ	36 (20–46)	56 (19–98)	68 (20–116)

0.029). Furthermore, a significant departure from randomness was apparent when applying the χ^2 test for contingency tables ($p_{tlc1} = 0.029$; $p_{est1} = 0.00071$). The data were fit to a generalized linear model using logistic regression (Figure 4E). At wt telomere length (300 nucleotides), the frequency of telomere elongation per round of DNA replication was 0.078 for *tlc1-Δ/TLC1* zygotes and 0.067 for *est1-Δ/EST1* zygotes. This frequency increased steadily to 0.46 for *tlc1-Δ/TLC1* zygotes and 0.42 for *est1-Δ/EST1* zygotes as telomeres shortened to 100 nucleotides. These data indicate that a typical telomere undergoes several rounds of semiconservative DNA replications without being elongated by telomerase. Therefore, telomeres switch between telomerase-extendible and -nonextendible states. The equilibrium between the two states is regulated by telomere length.

Telomere Length-Dependent Control of Extendibility at a Natural Telomere

Natural yeast telomeres contain in their subtelomeric region repetitive elements that are referred to as X and Y′, whereas the tagged telomere VR lacks these elements. To test if the above telomere elongation analysis of tagged VR could be extrapolated to natural telomeres, we analyzed telomere 1L, which contains an X element in its subtelomeric region. For this telomere, we had previously identified a unique subtelomeric sequence allowing specific amplification by telomere PCR (Teixeira et al., 2002). In order to amplify 1L from the recipient strain only, telomere IL of the donor strain was truncated and replaced with an artificial telomere (*tel IL::URA3*; see Supplemental Data at http://www.cell.com/cgi/content/full/117/3/323/DC1).

Parental *est1-Δ* IL telomeres were sequenced after 30 generations of clonal expansion to determine telomerase-independent events (Figure 3C). Divergence was observed in four out of 39 sequenced telomeres. All four diverging chromosome ends corresponded to telomeres that had shortened to near or below 100 nucleotides (Figure 3C), suggesting that telomerase-independent recombination may be regulated at this natural telomere in a length-dependent manner. These *est1-Δ* cells were mated with *EST1 tel IL::URA3* donor cells, and intact telomere IL was amplified as above (Figure 4C). As for telomere VR, the frequency of telomerase-dependent elongation events increased with telomere shortening ($r = -0.75$, $p_{pearson} = 0.020$, $\rho = -0.82$, $p_{spearman} = 2.75e-05$) (Figure 4E). Furthermore, a significant departure from randomness was apparent when applying the χ^2 test for contingency tables ($p_{tel1L} = 0.036$). The extent of elongation, as for telomere VR, did not convincingly correlate with telomere length ($r = -0.45$, $p_{pearson} = 0.058$; $\rho = -0.52$, $p_{spearman} = 0.029$) for telomeres longer than 120 nucleotides (Figure 4D).

Rif1p and Rif2p Regulate the Equilibrium between Extendible and Nonextendible Telomeric States

The Rif1 and Rif2 proteins are recruited to telomeres via the Rap1p C-terminal domain and are thought to mediate the Rap1-counting mechanism of telomere length control (Marcand et al., 1997). Simultaneous deletion of *RIF1* and *RIF2* has a synergistic effect on telomere length, indicating that they have distinct regulatory functions (Wotton and Shore, 1997). To better understand the mechanism of action of Rif1p, we mated a presenescent *rif1-Δ est1-Δ* strain with a *rif1-Δ EST1* strain and analyzed telomere elongation as described above (Figure 5). After 30 generations of clonal expansion, telomeres in the parental *est1-Δ rif1-Δ* strain had been extended by telomerase-independent elongation at a frequency of 23% (25 out of 110) (Figure 3F). Most of these events corresponded to telomeres that had shortened below 120 nucleotides. In the *rif1-Δ/rif1-Δ est1-Δ/EST1* zygote, telomere elongation frequency increased significantly ($p = 0.0084$) by approximately 2-fold when compared to the *est1-Δ/EST1* zygote, considering the telomeres that were longer than 120 nucleotides (Figure 5D). This indicates that Rif1p promotes formation of a telomere structure that prevents the productive association of telomerase. For telomeres that had shortened below 120 nucleotides, the high recombination background did not allow identification of telomerase-dependent elongation events without ambiguity. However, comparison of the frequency and length of extension in the presence and absence of telomerase (compare Figures 5A to Figure 3F) suggested that telomerase-mediated extension events contributed substantially to the observed elongation of short telomeres.

We also analyzed the extent of telomere elongation (Figure 5C) as a function of telomere length. As seen in *est1-Δ/EST1* zygotes, the telomere extensions were heterogeneous in size, ranging from ten to 261 nucleotides for the telomeres that had not shortened below 120 nucleotides. The average extension length was 83 nucleotides, with an interquartile range from 32 to 96. In the absence of Rif1p, the frequency of elongation ($r = -0.68$, $p_{pearson} = 6.04e-6$, $\rho = -0.62$, $p_{spearman} = 8.17e-5$) but not the extent of elongation ($r = -0.40$, $p_{pearson} = 0.09$, $\rho = -0.23$, $p_{spearman} = 0.37$) correlated significantly with telomere length (for telomeres that were longer than 120 nucleotides). In telomeres with a nearly physiological length of above 200 nucleotides, the *rif1-Δ* zygotes displayed a slightly longer extension length than *RIF1* controls (59 versus 44 nucleotides; see Table 1).

The effects of a *rif2* deletion were analyzed as for *rif1* (Figure 5B and Table 1). The frequency of telomere elongation increased similarly for *rif2-Δ* by approximately 2-fold when compared to *RIF2* cells, whereas the extension length was not affected (Table 1). As for *rif1-Δ*, the frequency ($r = -0.83$, $p_{pearson} = 0.04$, $\rho = -0.75$, $p_{spearman} = 0.0083$) but not the extent of telomere elongation ($r = -0.28$, $p_{pearson} = 0.234$, $\rho = -0.26$, $p_{spearman} = 0.275$) correlated significantly with telomere length. However, in contrast to *rif1-Δ* cells, the recombination background in *rif2-Δ* cells was, with four out of 63 analyzed telomeres, low and comparable to *RIF2* cells (Figure 3G), allowing a more straightforward assessment of telomerase-mediated events also for short telomeres. In conclusion, the data indicate that in *rif1-Δ* and *rif2-Δ* cells, telomeres are longer because they become more frequently extended by telomerase. Thus, both Rif1p and Rif2p control the productive association of the telomere substrate with telomerase.

Discussion

Telomere length homeostasis is fundamental for the maintenance and propagation of stable chromosomes.

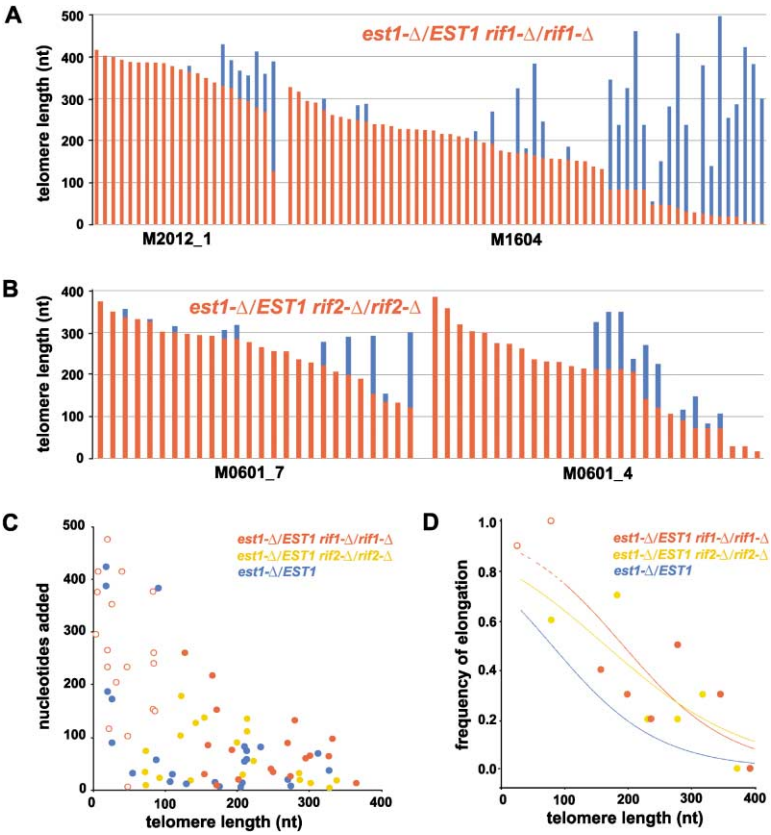

Figure 5. Frequency and Length of Telomere Extension as a Function of Telomere Size in *rif1*-Δ and *rif2*-Δ Cells

(A) Telomere elongation events in *est1*-Δ/*EST1 rif1*-Δ/*rif1*-Δ zygotes. YT56/*est1*-Δ cells were grown and mated with YT55 cells for 3 hr, and the tagged telomere at VR was analyzed. Two independent experiments (M2012_1 and M1604) are depicted on the left and right sides. Labeling is as in Figure 2.

(B) Same as (A) with *est1*-Δ/*EST1 rif2*-Δ/*rif2*-Δ zygotes.

(C) Length of telomere extension as a function of telomere size. The sizes of diverging regions obtained in the experiments described in (A) (red) and (B) (orange) are plotted as a function of the nondiverging sequence. The extension events in *est1*-Δ/*EST1* zygotes (blue) from Figure 4D are also indicated for comparison.

(D) Frequency of telomere extension as a function of telomere size. Sequences from (A) and (B) were analyzed as in Figure 4D. The plot corresponding to *est1*-Δ/*EST1* zygotes is reported from Figure 4D (blue). The $p_{\beta 1}$ value for *est1*-Δ/*EST1 rif1*-Δ/*rif1*-Δ zygotes is 2.45^{-5} and for *est1*-Δ/*EST1 rif2*-Δ/*rif2*-Δ is 0.0137. The curve corresponding to *est1*-Δ/*EST1 rif1*-Δ/*rif1*-Δ zygotes is dashed for telomeres below 100 nt, because, in this region, the events could not be attributed without ambiguity to telomerase-mediated extension, due to the high recombination background for short telomeres in the parent (see Figure 3F).

Loss of a single telomere is a potentially lethal event eliciting chromosome end fusions and missegregation. Previous work has indicated that telomerase activity is regulated in *cis* at individual telomeres through the number of double-stranded telomere binding proteins (Ancelin et al., 2002; Marcand et al., 1997; Ray and Runge, 1999a). This implies that telomeric chromatin controls either the enzymatic properties of telomerase, the accessibility of telomeric ends, or both (Marcand et al., 1999). To directly address and distinguish between these possibilities, we developed a method to measure telomere elongation events at single molecules. Our analysis demonstrates for the first time that telomerase does not act on every telomere in every cell cycle. We demonstrate the existence of at least two distinct telomeric states: one that allows the productive association with telomerase and one that prohibits telomerase-mediated telomere extension. We show that the frequency of telomere extension increases steadily as a function of telomere length, from roughly 6%–8% at 300 nucleotide-long telomeres to 42%–46% at 100 nucleotides. Thus, the equilibrium between the two states is regulated by telomere length. The existence of different telomeric states that prevent or permit telomerase access has been suggested, but direct experimental evidence for their existence was lacking.

Mechanism of Telomere Length Homeostasis

The telomere length dependent regulation of extendibility is sufficient to explain telomere length homeostasis (Figure 6). The nearly constant rate of telomere shortening due to incomplete end replication, nucleolytic processing, and telomere rapid deletion events is balanced by telomerase- and recombination-mediated telomere lengthening. A short telomere has a high probability of adopting the telomerase-extendible structure (Figure 6, lower). Upon elongation (Figure 6, upper), the equilibrium shifts to the nonextendible state, and the telomere's likelihood of being in the extendible state decreases with length. The average telomere length corresponds to the size at which the probability of extension multiplied by the average extension length equals the shortening rate. In *est1*Δ/*EST1* zygotes, the probability of extension at the wt telomere length of 300 nucleotides (0.067) multiplied by the average extension length (44 nucleotides for telomeres $>$200 nucleotides; Table 1) matches the measured shortening rate of 2.95 $\pm$ 0.2 nucleotides per generation (Marcand et al., 1999).

Our analysis of telomere sequence divergence in telomerase-negative cells (Figure 3) also indicates that recombination is contributing to telomere maintenance. The contribution of this pathway to telomere maintenance was detected in the telomerase-negative cells after clonal expansion for approximately 30 generations. At this time point, approximately 6% of the telomeres had undergone telomerase-independent elongation, corresponding to an estimated frequency of less than 0.3% per generation (Lea and Coulson, 1949). Thus, we estimate that the contribution of recombination to telomere maintenance is 20- to 30-fold lower than that of telomerase. The frequency of telomere recombination strongly increased in the *rif1*-Δ background for short

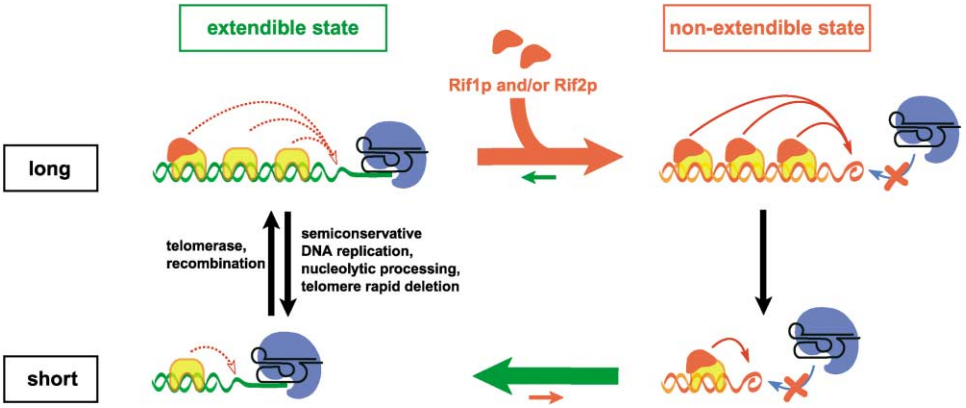

Figure 6. Model for Telomere Length Homeostasis

Telomeres exist in an equilibrium between two states: one that is extendible by telomerase (left side) and one that is nonextendible (right side). Long telomeres have a higher probability to be in the nonextendible state (upper part). As telomere length declines, the equilibrium between the two states shifts continuously to the extendible state (lower part). The average telomere length corresponds to the size at which the ratio of extendible over nonextendible states (probability of extension) multiplied by the average extension length equals the shortening rate. Rif1p and Rif2p, which associate with telomere bound Rap1p, promote the nonextendible state, shifting the equilibrium to the right. They may promote conformational changes of the telomeric 3′ end that prevent telomerase access or activation.

telomeres (Figure 3F). Interestingly, Rif1p was previously identified as a factor that inhibits type II recombination (Teng et al., 2000), a pathway that involves homologous recombination, which can be observed in a small fraction of yeast that escaped the lethality caused by telomerase loss. However, deletion of *RIF2* did not enhance telomerase-independent elongation in our study, while it favored the occurrence of type II survivors even more strongly than *rif1*-Δ (Teng et al., 2000).

The number of nucleotides added by telomerase varied substantially between individual telomerase extension events and was not tightly regulated by telomere length unless they were shorter than 100 nucleotides. However, telomeres of this size are unlikely to occur in wt yeast cells. The average length of the *ADE2*-tagged VR is 291 nucleotides, with a standard deviation of ±31 nucleotides (Forstemann et al., 2000). Thus, for the telomere size range of telomerase-positive cells, the extent of the elongation by telomerase does not correlate with the length of the original telomere. We conclude that under normal conditions, telomere length does not significantly control telomerase processivity or turnover. On the other hand, dramatic telomere shortening may remove telomere binding factors that block excessive elongation by telomerase, or a distinct pathway for the healing of severely shortened telomeres may become activated.

The mechanism for length homeostasis described here has interesting similarities and dissimilarities with another terminal nucleotide transferase, poly(A) polymerase, which polyadenylates mRNA precursors by adding approximately 250 nucleotides to precleaved mRNA molecules. Similarly to telomeres, poly(A) tail extension is regulated in *cis* by the number of bound nuclear poly(A) binding proteins (PABPN1) associated with the growing tail (Wahle, 1991). However, in contrast to double-stranded telomere binding proteins, PABPN1 do not regulate the initial binding of poly(A) polymerase but rather the processivity during extension. When the tail is short, PABPN1 stimulates the processivity of poly(A) polymerase. Upon reaching the natural length of approximately 250 nucleotides, the poly(A) binding protein loses its stimulating activity, and poly(A) polymerase switches from a processive to a distributive mode of extension (Wahle, 1991).

Yeast telomerase associates in vitro with telomeric primers in a stable manner and is able to add only a single telomeric repeat (Cohn and Blackburn, 1995; Prescott and Blackburn, 1997). Thus, our in vivo analysis indicates that additional factors must exist that either promote a processive mode of elongation or that enable rapid turnover of the enzyme. The described assay system provides a tool to identify processivity factors. A potential candidate might be the Est1p protein, which has been proposed to promote enzyme turnover or processivity (Singh and Lue, 2003). However, in our analysis, *est1*-Δ cells were indistinguishable from *tlc1*-Δ cells, being unable to add even a single telomeric repeat (Figure 4). We also determined telomere addition in *est1-60* cells, which express mutant Est1p with a single Lys → Glu mutational change at residue 444 (data not shown). This mutation disrupts an electrostatic interaction with Cdc13p, causing an ever-shorter telomeres phenotype (Pennock et al., 2001). In our analysis, this allele was, as *est1*-Δ, completely inactive in telomere addition. Thus, Est1p cannot act solely by promoting processivity or turnover but is also involved in the initial elongation cycle consistent with its function in telomerase recruitment (Evans and Lundblad, 1999; Pennock et al., 2001).

Rif1p and Rif2p Promote Formation of the Nonextendible Telomeric State

We identify the Rif1 and Rif2 proteins as critical mediators of the state of telomere extendibility. In both *rif1* and *rif2* mutant cells, the average telomere length increases, because the equilibrium between the extendible and nonextendible state is shifted (Figure 5). The extent of telomere elongation did not increase significantly with telomere shortening (Figure 5C).

How do Rif1p and Rif2p promote the nonextendible

state and prevent the productive association of telomerase with the telomere 3′ end in a length-dependent manner? The Rap1p-Rif1p and -Rif2 complexes might mediate their effects by favoring the formation of alternative DNA structures such as G quartets, which are known to prohibit telomerase extension in vitro (Zahler et al., 1991). Interestingly, Rap1p is known to promote G quartet formation in vitro (Giraldo et al., 1994). Another telomerase-inaccessible DNA structure could be provided through t loops, which have been described in vertebrates and protozoa, and in which the telomeric 3′ overhang is tucked away by forming a displacement loop with the telomere-proximal region (Griffith et al., 1999; Munoz-Jordan et al., 2001; Murti and Prescott, 1999). Experimental evidence for fold-back structures also exists in *S. cerevisiae*, but the status of the 3′ end in these structures is unknown (de Bruin et al., 2001; Strahl-Bolsinger et al., 1997). If this fold-back structure were to prevent telomerase access, one would predict that mutations in Sir proteins, which have been shown to disrupt this structure, should lead to a dramatic increase in telomere length. However, telomere length in *sir* mutants is slightly shorter than in wt cells (Palladino et al., 1993). It is also possible that Rif1p and Rif2p stimulate the telomere association of Cdc13p complexes, which may not only act as positive but also as negative regulators of telomere length (see, e.g., Chandra et al., [2001] and Grandin et al. [2001]). A similar mechanism has been proposed for human cells in which TRF1 may transmit its telomerase inhibition via the single-strand end binding protein POT1 (Loayza and De Lange, 2003), while, under other conditions, POT1 may stimulate telomerase activity (Colgin et al., 2003).

In summary, our data demonstrate that telomere length homeostasis is mediated through the telomere substrate, which is subject to a structural switch that regulates its productive association with telomerase. The described experimental system provides a means of deciphering which telomere-length regulators affect the equilibrium of the two telomeric states and ultimately will allow definition of their molecular natures.

Experimental Procedures

Mating of Yeast Cells

Telomerase-negative isolated transformants were inoculated in 50 ml of synthetic medium lacking histidine and grown overnight to a density of 10^8 cells/ml, as determined by cell counting. 10^8 recipient cells were mixed with 10^9 exponentially growing telomerase-positive donor cells. The mixtures were immediately concentrated by filtering on four membranes with a diameter of 47 mm each and a pore size of 0.8 μm (type AA from Millipore). Membranes were placed on prewarmed YPD plates at 30°C. After 3 hr, cells were resuspended by vigorous vortexing in 30 ml of synthetic medium lacking histidine and leucine. Ten milliliters of this suspension was diluted to 40 ml in the same selective medium and incubated at 30°C under agitation to allow diploids to grow for an additional 2 to 4 hr (5 and 7 hr after initial mixing, respectively). At each time point (0, 3, 5, and 7 hr after initial mixing), aliquots of the suspensions were analyzed. Genomic DNA was prepared from at least 5×10^7 of each of the parental cells and approximately 10^9 cells from mating mixtures. Mating efficiency was estimated by inspection of the cell mixtures under the microscope at the 3 hr time point. A spot assay on synthetic medium lacking either leucine, histine, or both was performed to quantify mating efficiency and to quantify the initial proportion of recipient cells and donor cells. DNA content was measured by fluorocytometry as described (Henchoz et al., 1997).

Telomere Sequencing and Analysis

Genomic DNA was extracted using the Wizard Genomic Kit (Promega). Total genomic DNA (30–100 ng) was used for telomere PCR as described (Forstemann et al., 2000). Briefly, genomic DNA was tailed with dCTP and terminal transferase. Telomeres were amplified using a primer (5′-TGTCCGAATTGATCCCAGAG-3′) that hybridized specifically to the *ADE2* gene at the telomere of chromosome VR of the recipient strains and with a primer (5′-$CGGGATCCG_{18}$-3′) complementary to the oligo-dC tail (see Figure 1B). For amplifying telomeres of chromosome 1L, a primer (5′-GCGGTACCAGGGTTA GATTAGGGCTG-3′) specific for the subtelomeric sequence of this chromosome was used. PCR products were separated on 2.5% preparative agarose gels, purified with a gel extraction kit (Qiagen), and cloned into the pDrive cloning vector using the PCR Cloning Plus Kit (Qiagen). Plasmid DNA was prepared from overnight cultures using the Millipore Montage Plasmid $Miniprep_{96}$ Kit. Plasmid DNA was sequenced using M13 forward or reverse primers and the SequiTherm EXCEL II DNA Sequencing Kit (Epicentre Technologies, Madison, WI) on a LiCor DNA Sequencer. Sequences were aligned, and sequence divergence was detected using the contig assembler of Sequencher (Gene Codes Corporation) or by analyzing the sequencing gel image directly.

Statistical Analysis

Package R v1.8.1 (Ihaka and Gentleman, 1996) was used for standard parametric and nonparametric tests. Telomeres were ordered according to their nondiverging size, and subgroups containing 10 telomeres were formed. The average telomere size of each subgroup was calculated and the frequency of elongation determined. The relationship between frequency of initiation and mean length of telomere of each subgroup was modeled using logistic regression. Several diagnostics were applied to test for lack of fit, outliers, and leverage points.

Acknowledgments

We thank K. Förstemann, J. Promisel Cooper, and the referees for helpful comments on the manuscript; K. Förstemann and S. Marcand for discussion; S. van der Straten for DNA sequencing; E. Schwob, V. Lundblad, and S. Marcand for plasmids; and B. Dujon for yeast strains. M.T.T. was the recipient of a postdoctoral fellowship from the Human Frontier Science Program. This work was supported by a Human Frontier Science Program grant and the Swiss National Science Foundation.

Received: July 23, 2003
Revised: February 17, 2004
Accepted: March 3, 2004
Published: April 29, 2004

References

Ancelin, K., Brunori, M., Bauwens, S., Koering, C.E., Brun, C., Ricoul, M., Pommier, J.P., Sabatier, L., and Gilson, E. (2002). Targeting assay to study the *cis* functions of human telomeric proteins: evidence for inhibition of telomerase by TRF1 and for activation of telomere degradation by TRF2. Mol. Cell. Biol. *22*, 3474–3487.

Barnett, M.A., Buckle, V.J., Evans, E.P., Porter, A.C., Rout, D., Smith, A.G., and Brown, W.R. (1993). Telomere directed fragmentation of mammalian chromosomes. Nucleic Acids Res. *21*, 27–36.

Bodnar, A.G., Ouellette, M., Frolkis, M., Holt, S.E., Chiu, C.-P., Morin, G.B., Harley, C.B., Shay, J.W., Lichtsteinter, S., and Wright, W.E. (1998). Extension of life-span by introduction of telomerase into normal human cells. Science *279*, 349–352.

Bryan, T.M., Englezou, A., Gupta, J., Bacchetti, S., and Reddel, R.R. (1995). Telomere elongation in immortal human cells without detectable telomerase activity. EMBO J. *14*, 4240–4248.

Bucholc, M., Park, Y., and Lustig, A.J. (2001). Intrachromatid excision of telomeric DNA as a mechanism for telomere size control in *Saccharomyces cerevisiae*. Mol. Cell. Biol. *21*, 6559–6573.

Cawthon, R.M., Smith, K.R., O'Brien, E., Sivatchenko, A., and Kerber,

R.A. (2003). Association between telomere length in blood and mortality in people aged 60 years or older. Lancet *361*, 393–395.

Chan, S., Chang, J., Prescott, J., and Blackburn, E. (2001). Altering telomere structure allows telomerase to act in yeasts lacking ATM kinases. Curr. Biol. *11*, 1240–1250.

Chandra, A., Hughes, T.R., Nugent, C.I., and Lundblad, V. (2001). Cdc13 both positively and negatively regulates telomere replication. Genes Dev. *15*, 404–414.

Cohn, M., and Blackburn, E.H. (1995). Telomerase in yeast. Science *269*, 396–400.

Colgin, L.M., Baran, K., Baumann, P., Cech, T.R., and Reddel, R.R. (2003). Human POT1 facilitates telomere elongation by telomerase. Curr. Biol. *13*, 942–946.

Conrad, M., Wright, J., Wolf, J., and Zakian, V. (1990). RAP1 protein interacts with yeast telomeres in vivo: overproduction alters telomere structure and decreases chromosome stability. Cell *63*, 739–750.

Cooper, J.P., Nimmo, E.R., Allshire, R.C., and Cech, T.R. (1997). Regulation of telomere length and function by a Myb-domain protein in fission yeast. Nature *385*, 744–747.

de Bruin, D., Zaman, Z., Liberatore, R.A., and Ptashne, M. (2001). Telomere looping permits gene activation by a downstream UAS in yeast. Nature *409*, 109–113.

Diede, S.J., and Gottschling, D.E. (1999). Telomerase-mediated telomere addition in vivo requires DNA primase and DNA polymerases alpha and delta. Cell *99*, 723–733.

Dunham, M.A., Neumann, A.A., Fasching, C.L., and Reddel, R.R. (2000). Telomere maintenance by recombination in human cells. Nat. Genet. *26*, 447–450.

Evans, S.K., and Lundblad, V. (1999). Est1 and Cdc13 as comediators of telomerase access. Science *286*, 117–120.

Evans, S.K., and Lundblad, V. (2000). Positive and negative regulation of telomerase access to the telomere. J. Cell Sci. *113*, 3357–3364.

Ferreira, M.G., Miller, K.M., and Cooper, J.P. (2004). Indecent exposure: when telomeres become uncapped. Mol. Cell *13*, 7–18.

Forstemann, K., and Lingner, J. (2001). Molecular basis for telomere repeat divergence in budding yeast. Mol. Cell. Biol. *21*, 7277–7286.

Forstemann, K., Hoss, M., and Lingner, J. (2000). Telomerase-dependent repeat divergence at the 3′ ends of yeast telomeres. Nucleic Acids Res. *28*, 2690–2694.

Giraldo, R., Suzuki, M., Chapman, L., and Rhodes, D. (1994). Promotion of parallel DNA quadruplexes by a yeast telomere binding protein: a circular dichroism study. Proc. Natl. Acad. Sci. USA *91*, 7658–7662.

Grandin, N., Damon, C., and Charbonneau, M. (2001). Ten1 functions in telomere end protection and length regulation in association with Stn1 and Cdc13. EMBO J. *20*, 1173–1183.

Griffith, J.D., Comeau, L., Rosenfield, S., Stansel, R.M., Bianchi, A., Moss, H., and de Lange, T. (1999). Mammalian telomeres end in a large duplex loop. Cell *97*, 503–514.

Hardy, C.F., Sussel, L., and Shore, D. (1992). A RAP1-interacting protein involved in transcriptional silencing and telomere length regulation. Genes Dev. *6*, 801–814.

Harley, C.B., Futcher, A.B., and Greider, C.W. (1990). Telomeres shorten during ageing of human fibroblasts. Nature *345*, 458–460.

Hemann, M.T., Strong, M.A., Hao, L.Y., and Greider, C.W. (2001). The shortest telomere, not average telomere length, is critical for cell viability and chromosome stability. Cell *107*, 67–77.

Henchoz, S., Chi, Y., Catarin, B., Herskowitz, I., Deshaies, R.J., and Peter, M. (1997). Phosphorylation- and ubiquitin-dependent degradation of the cyclin-dependent kinase inhibitor Far1p in budding yeast. Genes Dev. *11*, 3046–3060.

Huffman, K.E., Levene, S.D., Tesmer, V.M., Shay, J.W., and Wright, W.E. (2000). Telomere shortening is proportional to the size of the G-rich telomeric 3′-overhang. J. Biol. Chem. *275*, 19719–19722.

Jacob, N.K., Kirk, K.E., and Price, C.M. (2003). Generation of telomeric G strand overhangs involves both G and C strand cleavage. Mol. Cell *11*, 1021–1032.

Kelleher, C., Teixeira, M.T., Forstemann, K., and Lingner, J. (2002). Telomerase: biochemical considerations for enzyme and substrate. Trends Biochem. Sci. *27*, 572–579.

Kim, N.W., Piatyszek, M.A., Prowse, K.R., Harley, C.B., West, M.D., Ho, P.L., Coviello, G.M., Wright, W.E., Weinrich, S.L., and Shay, J.W. (1994). Specific association of human telomerase activity with immortal cells and cancer. Science *266*, 2011–2015.

Kim, S.H., Kaminker, P., and Campisi, J. (1999). TIN2, a new regulator of telomere length in human cells. Nat. Genet. *23*, 405–412.

Lea, D.E., and Coulson, C.A. (1949). The distribution of the numbers of mutants in bacterial populations. J. Genet. *49*, 264–285.

Li, B., and Lustig, A.J. (1996). A novel mechanism for telomere size control in *Saccharomyces cerevisiae*. Genes Dev. *10*, 1310–1326.

Lingner, J., Cooper, J.P., and Cech, T.R. (1995). Telomerase and DNA end replication: no longer a lagging strand problem? Science *269*, 1533–1534.

Loayza, D., and De Lange, T. (2003). POT1 as a terminal transducer of TRF1 telomere length control. Nature *424*, 1013–1018.

Lundblad, V., and Blackburn, E.H. (1993). An alternative pathway for yeast telomere maintenance rescues *est1*-senescence. Cell *73*, 347–360.

Lundblad, V., and Szostak, J.W. (1989). A mutant with a defect in telomere elongation leads to senescence in yeast. Cell *57*, 633–643.

Lustig, A., Kurtz, S., and Shore, D. (1990). Involvement of the silencer and UAS binding protein Rap1 in regulation of telomere length. Science *250*, 549–553.

Ihaka, R., and Gentleman, R. (1996). R: A language for data analysis and graphics. J. Comp. Graph. Stat. *5*, 299–314.

Makarov, V.L., Hirose, Y., and Langmore, J.P. (1997). Long G tails at both ends of human chromosomes suggest a C strand degradation mechanism for telomere shortening. Cell *88*, 657–666.

Marcand, S., Gilson, E., and Shore, D. (1997). A protein-counting mechanism for telomere length regulation in yeast. Science *275*, 986–990.

Marcand, S., Brevet, V., and Gilson, E. (1999). Progressive cis-inhibition of telomerase upon telomere elongation. EMBO J. *18*, 3509–3519.

Marcand, S., Brevet, V., Mann, C., and Gilson, E. (2000). Cell cycle restriction of telomere elongation. Curr. Biol. *10*, 487–490.

McEachern, M.J., and Blackburn, E.H. (1995). Runaway telomere elongation caused by telomerase RNA gene mutations. Nature *376*, 403–409.

McElligott, R., and Wellinger, R.J. (1997). The terminal DNA structure of mammalian chromosomes. EMBO J. *16*, 3705–3714.

Mitchell, J.R., Wood, E., and Collins, K. (1999). A telomerase component is defective in the human disease dyskeratosis congenita. Nature *402*, 551–555.

Munoz-Jordan, J.L., Cross, G.A., de Lange, T., and Griffith, J.D. (2001). t-loops at trypanosome telomeres. EMBO J. *20*, 579–588.

Murti, K.G., and Prescott, D.M. (1999). Telomeres of polytene chromosomes in a ciliated protozoan terminate in duplex DNA loops. Proc. Natl. Acad. Sci. USA *96*, 14436–14439.

Naito, T., Matsuura, A., and Ishikawa, F. (1998). Circular chromosome formation in a fission yeast mutant defective in two ATM homologues. Nat. Genet. *20*, 203–206.

Ouellette, M.M., Liao, M., Herbert, B.S., Johnson, M., Holt, S.E., Liss, H.S., Shay, J.W., and Wright, W.E. (2000). Subsenescent telomere lengths in fibroblasts immortalized by limiting amounts of telomerase. J. Biol. Chem. *275*, 10072–10076.

Palladino, F., Laroche, T., Gilson, E., Axelrod, A., Pillus, L., and Gasser, S.M. (1993). SIR3 and SIR4 proteins are required for the positioning and integrity of yeast telomeres. Cell *75*, 543–555.

Pennock, E., Buckley, K., and Lundblad, V. (2001). Cdc13 delivers separate complexes to the telomere for end protection and replication. Cell *104*, 387–396.

Prescott, J., and Blackburn, E.H. (1997). Telomerase RNA mutations

in *Saccharomyces cerevisiae* alter telomerase action and reveal nonprocessivity in vivo and in vitro. Genes Dev. *11*, 528–540.

Ray, A., and Runge, K.W. (1999a). Varying the number of telomere-bound proteins does not alter telomere length in *tel1*Δ cells. Proc. Natl. Acad. Sci. USA *96*, 15044–15049.

Ray, A., and Runge, K.W. (1999b). The yeast telomere length counting machinery is sensitive to sequences at the telomere-nontelomere junction. Mol. Cell. Biol. *19*, 31–45.

Ray, S., Karamysheva, Z., Wang, L., Shippen, D.E., and Price, C.M. (2002). Interactions between telomerase and primase physically link the telomere and chromosome replication machinery. Mol. Cell. Biol. *22*, 5859–5868.

Ritchie, K.B., Mallory, J.C., and Petes, T.D. (1999). Interactions of *TLC1* (which encodes the RNA subunit of telomerase), *TEL1*, and *MEC1* in regulating telomere length in the yeast *Saccharomyces cerevisiae*. Mol. Cell. Biol. *19*, 6065–6075.

Samper, E., Flores, J.M., and Blasco, M.A. (2001). Restoration of telomerase activity rescues chromosomal instability and premature aging in Terc$^{-/-}$ mice with short telomeres. EMBO Rep. *2*, 800–807.

Shore, D. (1997). Telomere length regulation: getting the measure of chromosome ends. Biol. Chem. *378*, 591–597.

Singh, S.M., and Lue, N.F. (2003). Ever shorter telomere 1 (*EST1*)-dependent reverse transcription by *Candida* telomerase in vitro: evidence in support of an activating function. Proc. Natl. Acad. Sci. USA *100*, 5718–5723.

Smith, S., and de Lange, T. (2000). Tankyrase promotes telomere elongation in human cells. Curr. Biol. *10*, 1299–1302.

Smogorzewska, A., and de Lange, T. (2004). Regulation of telomerase by telomeric proteins. Annu. Rev. Biochem. *73*, 177–208.

Smogorzewska, A., van Steensel, B., Bianchi, A., Oelmann, S., Schaefer, M.R., Schnapp, G., and de Lange, T. (2000). Control of human telomere length by TRF1 and TRF2. Mol. Cell. Biol. *20*, 1659–1668.

Strahl-Bolsinger, S., Hecht, A., Luo, K., and Grunstein, M. (1997). SIR2 and SIR4 interactions differ in core and extended telomeric heterochromatin in yeast. Genes Dev. *11*, 83–93.

Taggart, A.K., Teng, S.C., and Zakian, V.A. (2002). Est1p as a cell cycle-regulated activator of telomere-bound telomerase. Science *297*, 1023–1026.

Teixeira, M.T., Forstemann, K., Gasser, S.M., and Lingner, J. (2002). Intracellular trafficking of yeast telomerase components. EMBO Rep. *3*, 652–659.

Teng, S.C., and Zakian, V.A. (1999). Telomere-telomere recombination is an efficient bypass pathway for telomere maintenance in Saccharomyces cerevisiae. Mol. Cell. Biol. *19*, 8083–8093.

Teng, S., Chang, J., McCowan, B., and Zakian, V.A. (2000). Telomerase-independent lengthening of yeast telomeres occurs by an abrupt Rad50p-dependent, Rif-inhibited recombinational process. Mol. Cell *6*, 947–952.

van Steensel, B., and de Lange, T. (1997). Control of telomere length by the human telomeric protein TRF1. Nature *385*, 740–743.

Vulliamy, T., Marrone, A., Goldman, F., Dearlove, A., Bessler, M., Mason, P.J., and Dokal, I. (2001). The RNA component of telomerase is mutated in autosomal dominant dyskeratosis congenita. Nature *413*, 432–435.

Wahle, E. (1991). A novel poly(A)-binding protein acts as a specificity factor in the second phase of messenger RNA polyadenylation. Cell *66*, 759–768.

Wellinger, R.J., Ethier, K., Labrecque, P., and Zakian, V.A. (1996). Evidence for a new step in telomere maintenance. Cell *85*, 423–433.

Wotton, D., and Shore, D. (1997). Novel Rap1p-interacting factor, Rif2p, cooperates with Rif1p to regulate telomere length in *Saccharomyces cerevisiae*. Genes Dev. *11*, 748–760.

Wright, W.E., Tesmer, V.M., Huffman, K.E., Levene, S.D., and Shay, J.W. (1997). Normal human chromosomes have long G-rich telomeric overhangs at one end. Genes Dev. *11*, 2810–2821.

Zahler, A.M., Williamson, J.R., Cech, T.R., and Prescott, D.M. (1991). Inhibition of telomerase by G-quartet DNA structures. Nature *350*, 718–720.

Zhu, L.X., Hathcock, K.S., Hande, P., Lansdorp, P.M., Seldin, M.F., and Hodes, R.J. (1998). Telomere length regulation in mice is linked to a novel chromosome locus. Proc. Natl. Acad. Sci. USA *95*, 8648–8653.